

A physical model suggests that hip-localized balance sense in birds improves state estimation in perching: implications for bipedal robots

Darío Urbina-Meléndez^{1,4,§}, Kian Jalaeddini^{2,§}, Monica Daley³ and Francisco J Valero-Cuevas^{1,2,*}

¹*Department of Biomedical Engineering, University of Southern California, USA.*

²*Division of Biokinesiology and Physical Therapy, University of Southern California, USA.*

³*Comparative Biomedical Sciences, The Royal Veterinary College, UK.*

⁴*The School of Engineering, National Autonomous University of Mexico, Mexico.*

§*Contributed equally.*

Correspondence*:

Francisco J Valero-Cuevas

University of Southern California, Ronald Tutor Hall, RTH-421, 3710 S. McClintock Ave, Los Angeles, 90089-2905, California, United States
valero@usc.edu

2 ABSTRACT

3 In addition to a vestibular system, birds uniquely have a balance-sensing organ within the pelvis,
4 called the lumbosacral organ (LSO). The LSO is well developed in terrestrial birds, possibly
5 to facilitate balance control in perching and terrestrial locomotion. No previous studies have
6 quantified the functional benefits of the LSO for balance. We suggest two main benefits of
7 hip-localized balance sense: reduced sensorimotor delay and improved estimation of foot-ground
8 acceleration. We used system identification to test the hypothesis that hip-localized balance
9 sense improves estimates of foot acceleration compared to a head-localized sense, due to
10 closer proximity to the feet. We built a physical model of a standing guinea fowl perched on a
11 platform, and used 3D accelerometers at the hip and head to replicate balance sense by the
12 LSO and vestibular systems. The horizontal platform was attached to the end effector of a 6
13 DOF robotic arm, allowing us to apply perturbations to the platform analogous to motions of
14 a compliant branch. We also compared state estimation between models with low and high
15 neck stiffness. Cross-correlations revealed that foot-to-hip sensing delays were shorter than
16 foot-to-head, as expected. We used multi-variable output error state-space (MOESP) system
17 identification to estimate foot-ground acceleration as a function of hip- and head-localized sensing,
18 individually and combined. Hip-localized sensors alone provided the best state estimates, which
19 were not improved when fused with head-localized sensors. However, estimates from head-
20 localized sensors improved with higher neck stiffness. Our findings support the hypothesis that
21 hip-localized balance sense improves the speed and accuracy of foot state estimation compared
22 to head-localized sense. The findings also suggest a role of neck muscles for active sensing for

23 balance control: increased neck stiffness through muscle co-contraction can improve the utility of
24 vestibular signals. Our engineering approach provides, to our knowledge, the first quantitative
25 evidence for functional benefits of the LSO balance sense in birds. The findings support notions
26 of control modularity in birds, with preferential vestibular sense for head stability and gaze, and
27 LSO for body balance control, respectively. The findings also suggest advantages for distributed
28 and active sensing for agile locomotion in compliant bipedal robots.

29 **Keywords:** balance, lumbosacral organ, vestibular system, birds, perch, compliant robot, co-localized sensing, distributed sensing

1 INTRODUCTION

30 All terrestrial vertebrates have linear and angular acceleration sense localized to the vestibular system of the
31 inner ear. It is well known that birds use a variety of reflexes mediated by internal signals to stabilize their
32 head during walking and flying [1]. Uniquely among living animals, birds appear to have two specialized
33 balance-sensing organs: the vestibular system of the inner ear and an additional balance sensor located
34 between the hips called the lumbosacral organ (LSO) [2] which has been proposed to be especially useful
35 for terrestrial locomotion [2], [3].]] Birds have long flexible necks, with head motions tightly coupled
36 to gaze control [4, 5, 6]. Consequently, the vestibular system is not closely nor tightly coupled to the
37 torso. In contrast, the LSO is located in the sacrum between the hips, near the CoM. Having a balance
38 organ at the torso is likely to be beneficial to legged locomotion and balance because the hip joint plays an
39 important role on controlling the position of the CoM of the whole body with respect to the foot [7]. Here
40 we consider and contrast the functional implications of hip-localized (LSO) and head-localized (vestibular)
41 balance-sense.

42 Generally speaking, keeping balance is a task that many legged-animals perform to prevent falling or
43 rotating about the foot point after perturbations [8]. Specifically, a balance-sensing organ produces afferent
44 signals to detect current body posture and motion to determine the movements required to achieve or
45 maintain a desired posture and motion. In birds, direct neurophysiological evidence has clearly established
46 that they must possess balance sense that is independent of the vestibular system [7]. They retain the ability
47 to reflexively compensate for body rotations even after labyrinthectomy and spinal cord transection to
48 eliminate descending inputs influenced by the vision and vestibular senses [7]. This neurophysiological
49 evidence, along with particular anatomical features of avian lumbosacral region (below), suggests a balance
50 sensing function of the LSO that complements proprioceptive information from the vestibular system, as
51 well as mechanoreceptors in the skin, joints and muscles.

52 Anatomically, the LSO is located within an enlargement of the lumbosacral region of the spinal column,
53 between the 27th to 38th segments [9]. The LSO presents a suite of features unique to the spinal column of
54 birds, including bilateral protrusions of neural tissue identified as mechanosensors (accessory lobe (AL)
55 neurons), located adjacent to ligaments supporting the spinal cord [10], [11], [3], [2]. The spinal cord is
56 dorsally bifurcated in this region and supports a “glycogen body” (GB) centered on top. The entire region
57 is enclosed by bony canals with a distinct concentric ring structure [2]. The arrangement of the canals,
58 AL, ligaments, and GB is reminiscent of the vestibular system [2] and invites functional analogy to an
59 accelerometer. Each AL contains mechanoreceptors [2, 10, 11], with commissural axons projecting to
60 last-order premotor interneurons in the spinal pattern generating network [12, 2]. The AL neurons within
61 the LSO exhibit spontaneous firing and phase-coupled firing in response to vibrational stimulation between
62 75-100Hz, and ablation of these neurons disrupts standing balance [2]. Thus, multiple lines of anatomical
63 and neurophysiological evidence suggest balance-sensing function of the LSO.

64 Despite evidence of LSO hip-localized balance-sense in birds, no previous studies have provided
65 quantitative evidence for the functional benefits of LSO as an adaptation for posture balance sensing
66 of posture-relevant information. We hypothesize that hip-localized balance sense provides two main
67 functional advantages compared to head-only balance-sense: 1) reduced sensorimotor delay and 2) more
68 accurate state estimation of foot-ground acceleration due to closer proximity to the feet. Here we use a
69 physical model of a perching guinea fowl subject to foot-ground perturbations to test the hypothesis that
70 hip-localized balance sense enables more rapid sensing and accurate state estimation compared to only a
71 head-localized balance sense.

72 Most birds “perch” (balance with the feet attached to the substrate) when they alight on elevated objects
73 such as branches; therefore we focus on perching as a conveniently simple and ecologically relevant
74 balancing behavior. We built a simple physical model of a standing guinea fowl perched on a horizontal
75 platform (i.e., feet attached to the platform). The horizontal platform was attached to the end effector of a 6
76 DOF robotic arm, allowing us to apply perturbations analogous to motions of a compliant branch. The
77 physical model provides a first approximation of the muscle-tendon viscoelastic properties that provide leg
78 compliance. We approximated LSO and vestibular balance sensors using 3-D accelerometers located at
79 hips and at the head, respectively. We used system identification to estimate foot-ground acceleration as a
80 function of hip- and head-localized sensing, individually and combined.

2 MATERIALS AND METHODS

81 2.1 Physical model of a guinea fowl

82 A skeletal model of a guinea fowl was built by interconnected and hinged aluminum bars (Figure 1 and
83 2). Friction was reduced by using bearings at the hip, knee, ankle, and foot. The general body size, limb
84 segment lengths and configuration were based on guinea fowl anatomy from the literature [13, 14, 15],
85 with a hip height of 20 cm.

86 This physical model focused on approximating the guinea fowl’s (*i*) LSO (hip) and vestibular (head)
87 balance sensing systems location, (*ii*) body center of mass location, and limb configuration in a standing
88 posture (*iii*) visco-elastic mechanical properties of the muscle-tendon-driven limbs. This model was meant
89 as a first approximation of the key physical features, to allow a quantitative comparison of the information
90 available at hip- and head-localized balance sensors. It was not meant to be an exhaustive exploration of
91 the effects of posture, material properties, and muscle-tendon actions. Such considerations could be the
92 subject of future work.

93 The toes of the model were firmly attached to a platform. Thus, the guinea fowl model “perched” while
94 maintaining an upright standing posture. This posture was maintained by the passive tensions in rubber
95 bands that cross the hip, knee, ankle and metatarsal joints without further assistance or active support
96 (Figure 2). We pre-tensioned rubber bands across joints to represent the tendon-driven functional anatomy
97 of a guinea fowl. These rubber bands also have viscoelastic properties that approximate the passive
98 mechanical properties of “muscles” held at a constant activation level when holding the standing posture.
99 The origins and insertions of the rubber bands were adjusted to have large enough moment arms at each
100 joint to overcome gravity and maintain posture even when perturbed by the moving platform. Our focus
101 was not to explore effects of varying muscle activation patterns for standing postures, but instead to find a
102 set of tensions in the rubber bands sufficient to maintain standing posture and propagate the perturbations
103 from the platform through the skeletal anatomy.

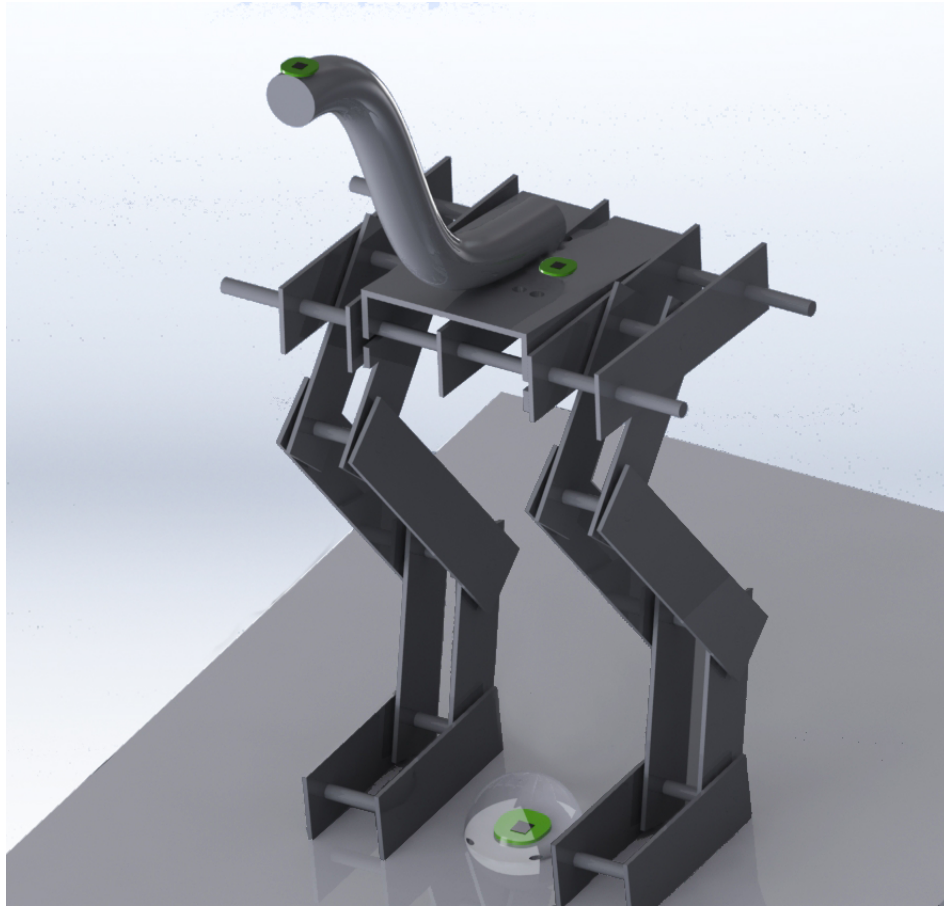


Figure 1. Physical model of the skeleton of the guinea fowl made of articulated aluminum plates and an elastic tube for a neck. The location of the sensors can be seen on the floor between the model's feet, on its pelvis between the hips, and on its head. The joints of the model are, starting from the pelvis: the hip, knee, ankle and metatarsal joints. The transparent sphere around the accelerometer between the feet indicates the scale of random displacements 20 mm in radius.

104 We used two interchangeable necks, each with different stiffness to test the effects of muscle coactivation
 105 on balance sensing at the head. Each neck was 25 cm long and curved as shown in Figure 1 and 2.
 106 The first neck was made of 12.7 mm diameter Ultra-Flex Corrugated Steel Sleaving (McMaster-Carr,
 107 part 54885K21). The second was 19.05 mm diameter Abrasion-Resistant Polyurethane Rubber Rod
 108 (McMaster-Carr, part 8695K155).

109 2.2 Instrumentation

110 The end-effector of a 6 degrees of freedom (DOF) AdeptSix 300 robotic arm (Omron Adept Technologies,
 111 Inc, San Ramón, CA) hold the platform where the model perched (Figure 3). We used 3-D accelerometers
 112 at the following locations on the model: (*i*) head to represent the vestibular system; (*ii*) hip to represent
 113 the LSO sensor, and (*iii*) between the feet to record the reference perturbations or "foot acceleration"
 114 (Figure 1). All accelerometers were MEMS inertial sensors Model LIS344ALH (ST Microelectronics,
 115 Geneva, Switzerland).



Figure 2. Photograph of the physical model of the skeleton of the guinea fowl. On the left the complete model is shown, on the middle and right sections details of the elastic linkages that are required for the robot to maintain a standing posture can be seen.

TRIALS	Low Stiffness neck	High Stiffness neck
2mm sphere	<i>Trial_LS₂</i>	<i>Trial_HS₂</i>
5mm sphere	<i>Trial_LS₅</i>	<i>Trial_HS₅</i>
10mm sphere	<i>Trial_LS₁₀</i>	<i>Trial_HS₁₀</i>
20mm sphere	<i>Trial_LS₂₀</i>	<i>Trial_HS₂₀</i>

Table 1. Each trial consisted of 3,000 random center-out-and-back displacements (center-surface of a sphere).

116 **2.3 Trials**

117 Each trial replicated a scenario that a guinea fowl might face while perching on a tree branch which is
 118 subject to perturbations from weather and other animals. Our goal was not to replicate natural perturbation
 119 exactly, but to provide a general test of our hypothesis that the LSO has benefits over the vestibular system
 120 for rapid and accurate state estimation for balance.

121 Each trial consisted of a series of 3,000 random, uncorrelated displacements generated by the robotic arm.
 122 Each displacement was a center-out-and-back movement in a random direction to the surface of spheres
 123 with 2, 5, 10, and 20 mm in radius. Trials were block-randomized across sphere sizes. We recorded a total
 124 of eight trials (4 sphere sizes x 2 necks stiffnesses) (Table 1).

125 **2.4 Data Acquisition**

126 We used a high-performance National Instruments (NI) *PXI-8108* computer, upgraded with 4 GB DDR2
 127 RAM and a 500 GB SSD. An NI *PXI-6254* ADC card recorded the accelerations signals. The data
 128 acquisition hardware was housed in the NI *PXI-1042* chassis. We acquired data at the sampling rate of
 129 1kHz.

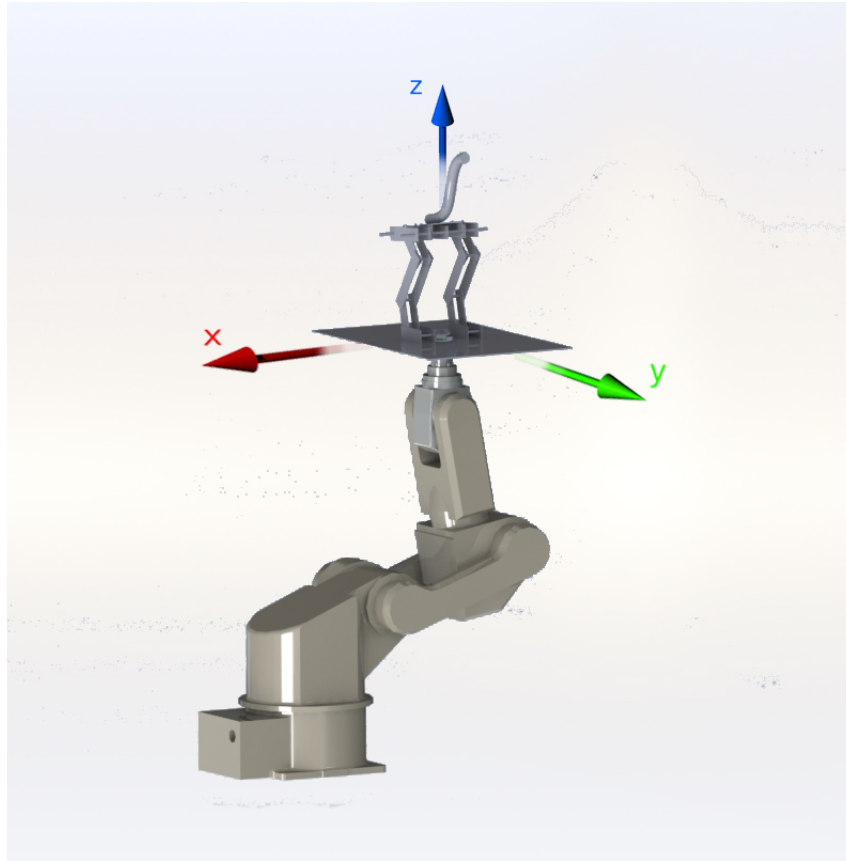


Figure 3. Generating 3D movements with the 6-DOF AdeptSix 300 robotic arm enabled us to apply repeatable and specific type of perturbations to our model.

130 2.5 Data Analysis

131 2.5.1 Estimation of neck stiffness

132 To estimate the effective neck stiffness, we performed a boot-strap analysis of 1,000 trials by randomly
 133 selecting 30s segments from each trial. We then found the resonant frequency (the frequency with maximal
 134 power) of accelerations at the head. The effective muscle stiffness was estimated from:

$$K_i = m_i f_i^2 \quad (1)$$

135 Where i is the neck number, m_i the mass and f_i the resonant frequency.

136 2.5.2 Estimation of sensory delay at the hip and head

137 We calculated cross-correlation of foot acceleration against that recorded from hip or head to estimate
 138 the propagation delays of the applied mechanical perturbations. The delay was taken as the lag where the
 139 cross-correlation was maximal.

140 2.5.3 Estimation of the time history of foot acceleration

141 We used a data-driven modeling approach to estimate the time history of the foot acceleration given the
 142 time history of signals recorded at the sensory sites (hip and head). To this end, we trained state-space
 143 models (in the least-squares sense) to predict foot acceleration from the hip or head accelerations. We used

144 MOESP state-space identification [16, 17] implemented in the *State-space Model Identification* (SMI)
 145 MATLAB toolbox [18]. The state-space model is represented as follows:

$$\begin{cases} x(k+1) &= Ax(k) + Bacc_{\text{sensor}}(k) \\ acc_{\text{foot}}(k) &= Cx(k) + Dacc_{\text{sensor}}(k) \end{cases} \quad (2)$$

146 where $acc_{\text{sensor}}(k)$ is the input signal (acceleration signal recorded from the hip or neck) and $acc_{\text{foot}}(k)$ is
 147 the measured foot acceleration. $x(k)$ is the state variable, and A, B, C, D are the unknown state-space
 148 matrices. We set the model order to three after inspecting the singular values of the extended observability
 149 matrix as described in the previous work [19]. The model order of three resulted in 21 parameters that was
 150 significantly less than the number of 4000 available training data points for each training run. Since the
 151 number of free parameters was much less than 10% of the training data, the model is not over-parameterized
 152 and cannot learn noise and the stochastic behavior.

153 We assessed the performance of the model in predicting the foot acceleration (\hat{acc}_{foot}). By running the
 154 identified models in the prediction mode, we compared the predictions to the actual measured signals,
 155 acc_{foot} . We quantified the difference using the identification *Variance Accounted For* (VAF) expressed as:

$$\%VAF = 100 \left(1 - \frac{\text{var}(\hat{acc}_{\text{foot}}(k) - acc_{\text{foot}}(k))}{\text{var}(acc_{\text{foot}}(k))} \right) \quad (3)$$

156 where 100% indicates a perfect prediction of all the variability in the measured signals, and 0% means no
 157 meaningful prediction.

158 2.5.4 Boot-Strap Analysis and Statistics

159 To estimate the robustness of the analyses (cross-correlation, system identification, etc), we performed a
 160 100 trials boot-strap study (random sampling with replacement) [20]. For each trial, we randomly chose 40s
 161 windows from the measured data, performed the cross-correlation and system identification analyses, and
 162 then calculated summary statistics across the 100 measures. We performed student's t-test for statistically
 163 significant differences between conditions. Values for central tendency and variance are reported as medians
 164 (interquartile range) unless stated otherwise.

3 RESULTS

165 We first present the differences in neck stiffness, then the effect of sensor location and neck stiffness on (i)
 166 sensing delay, and (ii) estimation of foot acceleration.

167 The necks made from two different materials have different bending stiffnesses whose estimates are
 168 shown in figure 4. Since we measured the dynamical response of the entire physical model (see Discussion),
 169 each direction and magnitude of perturbation induced a different dynamical response that resulted in a
 170 different acceleration measured at the head. This led to different resonant frequencies to be multiplied by
 171 the mass of the neck (Equation 1). Note that we would obtain different estimates of neck stiffnesses if the
 172 square of the resonant frequency at the head were multiplied by the mass of the whole model. Doing this
 173 would have given us an approximation of the stiffness of the whole body, which besides the neck, has a
 174 fixed stiffness. Also, if the complete body mass were considered, mass differences between trials with
 175 different necks would have been smaller, resulting in a constant bias that would not change the statistical
 176 differences between the estimates of neck stiffness. The median neck stiffnesses were 0.67 (0.26 to 1.05)

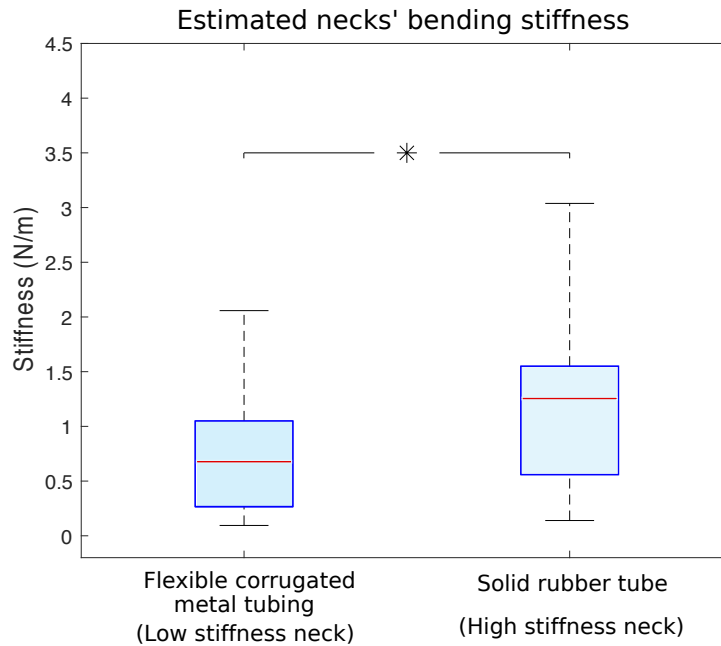


Figure 4. Estimated bending stiffness of the two necks. Neck stiffnesses were calculated using data from 1,000 different trials and the simple lumped-parameter model in Equation 1. Left: stiffness calculated for the flexible corrugated metal tubing (i.e., low stiffness neck). Right: stiffness calculated for the solid rubber tube (i.e., high stiffness neck) Flexible corrugated metal tubing and solid rubber tube data were statistically different (to $p < 0.05$), their respective medians are 0.67 and 1.25 N/m.

177 N/m and 1.25 (0.56 to 1.55) N/m for the low and high stiffness necks, respectively. Student t-test shows the
 178 average neck stiffness are significantly different ($p < 0.05$).

179 As expected, an accelerometer at the hip generally detected foot acceleration with shorter delays than the
 180 accelerometer at the head. Foot-to-hip median delays were 0.02 (0 to 0.03) s and 0.03 (0.005 to 0.065)
 181 s, respectively for the low and high stiffness necks. Foot-to-head median delays were longer, measured
 182 at 0.095 (0.06 to 0.135) s for the low stiffness neck, and 0.055 (0.02 to 0.07) s for the high stiffness
 183 one (Figure 5). The variability was quite large as the shown information collapses data across different
 184 acceleration axes and different sphere experiments (perturbation magnitudes).

185 Foot-to-hip delays were significantly shorter than foot-to-head delays ($p < 0.05$) for the low stiffness
 186 neck, but not significantly different for the high stiffness neck (Figure 5). A stiffer neck reduced the delays
 187 for information sensed at the head. This resulted in hip and neck delays that were very similar with no
 188 statistical difference.

189 Estimates of acceleration at the feet are more accurate when using signals from the hip-mounted
 190 accelerometers than from the head-mounted accelerometers. Figure 6 shows an example where acceleration
 191 at the feet is estimated from the hip- and head- mounted accelerometer, overlaid with the ground-truth
 192 signal measured at the feet.

193 Hip-localized estimates of the foot acceleration accounted for 30.81-48.96 % of variance (% VAF as
 194 defined in equation 3) against 15.59-22.19 % of head-localized estimates (Figure 7). This figure summarizes
 195 the estimation results by pooling together data from both neck stiffnesses. Prediction of foot acceleration
 196 as a function of neck type is shown in figure 8. Particularly, figure 7 shows data separated as a function of

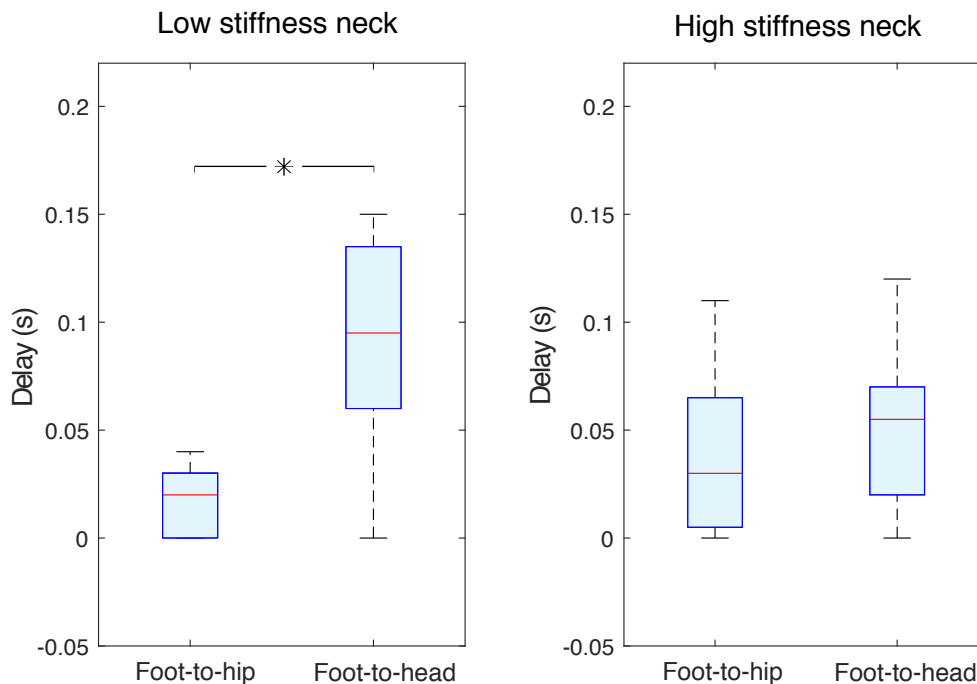


Figure 5. Independently of the neck stiffness, foot-to-hip delays were shorter than foot-to-head ones. The two data groups in the panel corresponding to the low stiffness neck (left panel) were statistically different (to $p < 0.05$); this is not the case for high stiffness neck data (right panel). Foot-to-head median delays were longer, measured at 0.095 s for the low stiffness neck, and 0.055 s for the high stiffness one. Foot-to-hip median delays were 0.02 and 0.03 s respectively for the low stiffness and high stiffness necks.

197 perturbation magnitude. It demonstrates that independently of the perturbation magnitude, the estimate of
 198 foot acceleration from the hip was always more accurate than that from the head sensor. Moreover, sensory
 199 fusion (combining info from both sensors) did not significantly improve the foot acceleration estimation.
 200 Therefore sensory fusion did not provide additional benefits beyond hip-only sensing.

201 We have found that when only head-localized accelerometers were available, the high stiffness neck
 202 improved estimates of foot acceleration compared to the low stiffness neck (Fig. 8). With the low stiffness
 203 neck, the median VAF was 15.11 (11.38 to 21.74) % , while it was 17.95 (10.18 to 29.19) % for the high
 204 stiffness one. These data groups were statistically different ($p < 0.05$).

DISCUSSION

205 To validate the anatomical and neurophysiological evidence of LSO balance sensing function in birds,
 206 we present a quantitative investigation of the functional benefits of hip-localized balance sense. Here we
 207 investigated the perturbation sensing dynamics of a physical model of a guineafowl perched in a standing
 208 posture. We explored two proposed functional advantages of hip-localized compared to head-localized
 209 balance sense: minimization of sensorimotor delay and improved estimation of foot-ground acceleration,
 210 due to closer proximity of the sensor to the feet. To our knowledge, this is the first study to quantitatively
 211 analyze the practical benefits of hip-localized sensing of accelerating for balance control. We find that a

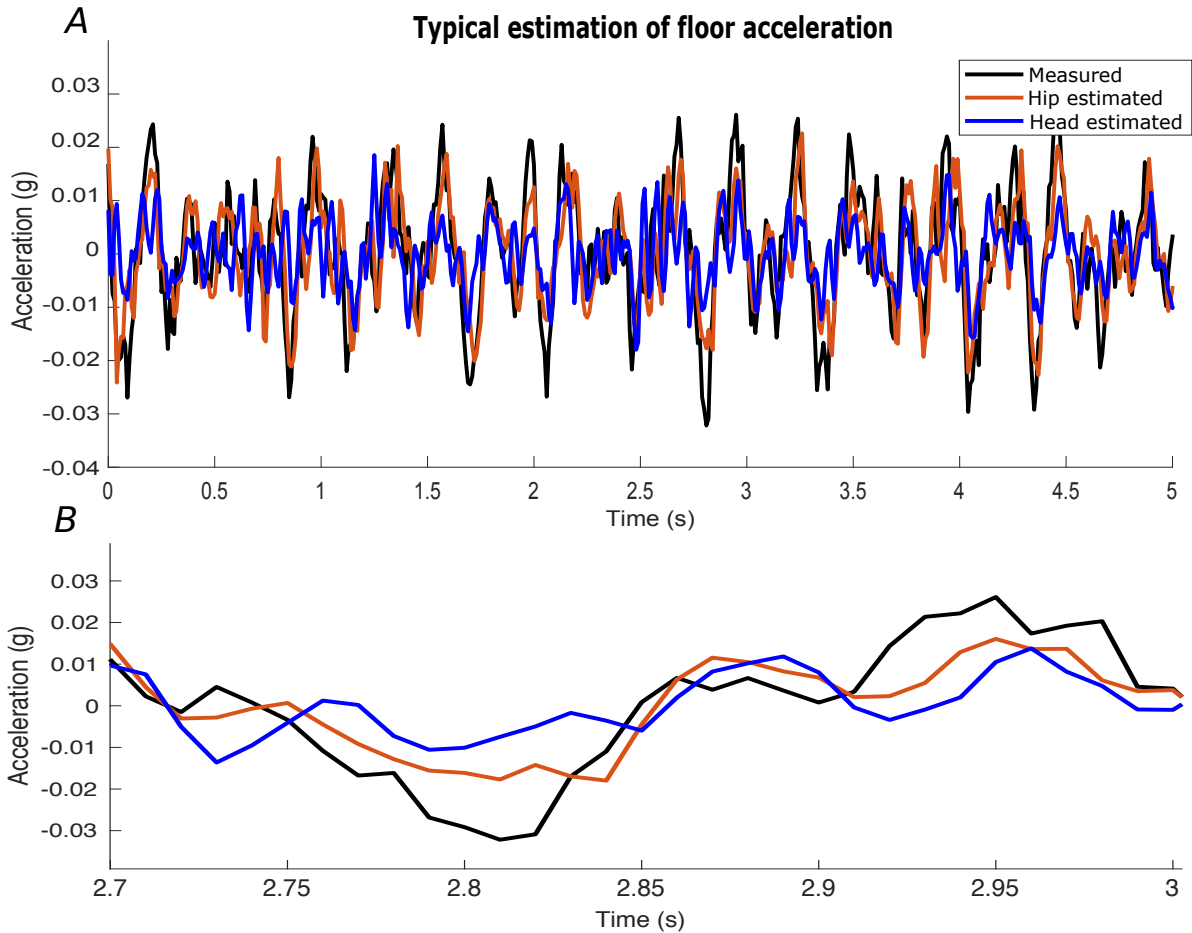


Figure 6. Example of the acceleration at the feet in the sagittal plane estimated from the measured accelerations at the hip and head. The acceleration at the hip yields more accurate estimates of acceleration at the feet. (A) a 5 (s) time window. (B) a 300 (ms) time window.

212 hip-localized acceleration sensor—analogue to the LSO—provides shorter delays and improved state
 213 estimation of feet acceleration during substrate perturbations.

214 In particular, our experimental paradigm applied displacements at the feet, where we also measured the
 215 ‘ground truth’ acceleration of the moving substrate on which the bird is perched. We then compared the
 216 ability to sense and reconstruct that ground truth acceleration on the basis of accelerations measured at the
 217 hip and head. We find that the location of these simulated balance sense organs has important consequences
 218 to how a bird (a model of a guinea fowl, in this case) could use acceleration information from hip-localized
 219 balance sense for bipedal perching, standing and locomotion. A second level of analysis focused on the
 220 material properties of the neck of the physical model. One was (less stiff) corrugated tubing, and the
 221 other (more stiff) solid rubber tubing. These material differences were designed to explore the effect of
 222 muscle co-contraction at the neck as a means of active sensing, or at least modulation of the utility of
 223 head-localized balance sense.

224 Before discussing the results in detail, it is important to clarify some features of our experimental
 225 approach to balance sense. A salient feature of our experimental results is the variability in our results, as in

Estimation of foot acceleration

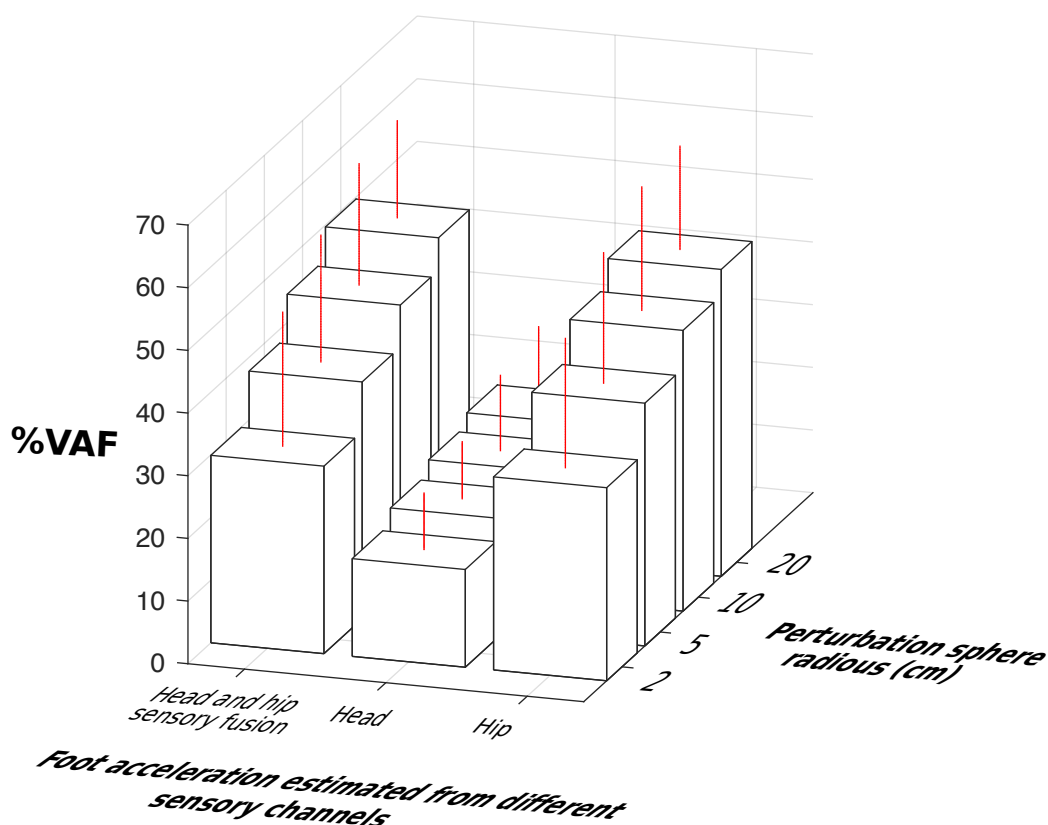


Figure 7. Comparison of estimation accuracy of foot acceleration from the hip, head and their fusion as a function of perturbation magnitudes. Hip-to-feet compared to head-to-foot acceleration estimation was more accurate ($p < 0.05$). Fusion of the hip and head information did not improve estimation of the foot acceleration beyond that obtained with hip information along.

226 Figure 4. Shouldn't the bending stiffness of each neck be thought as a single number? Similarly, shouldn't
 227 the foot-to-hip delays be constant and the same independently of neck stiffness (Figure 5)? Recall that the
 228 stiffness of the system is inferred from the resonant frequency of the acceleration measured at the head.
 229 The acceleration at the head is a function of the the dynamical response of the entire guinea fowl model to
 230 input perturbations. In fact, we are measuring the frequency response and delays of the coupled oscillations
 231 of the legs held in a standing position by rubber bands, plus the pelvis and neck. Given that this physical
 232 structure is only symmetric in the sagittal plane, its dynamical response will depend on the direction of the
 233 3D perturbations—which naturally results in variability in our results. Nevertheless, the corrugated tubing
 234 condition ('low stiffness neck') leads to perturbation responses at the head that, in general and on average,
 235 reflect a lower stiffness for this lumped-parameter analysis. Similarly, foot-to-hip delays were, in general
 236 and on average, shorter than the feet-to-head delays. In a sense, instead of 'neck stiffness,' the results in
 237 Figure 4 may be better called the 'apparent stiffness lumped at the head.' But given that the purpose of
 238 this analysis is to test for the effect of the material properties of the neck on time delays and estimation
 239 accuracy, we chose not to belabor this point and simply call it 'neck stiffness.' After all, (i) the neck is the
 240 only body part that was swapped, and (ii) changes in material properties only at the neck better reflect the
 241 potential effects of muscle co-contraction at the neck in the guinea fowl.

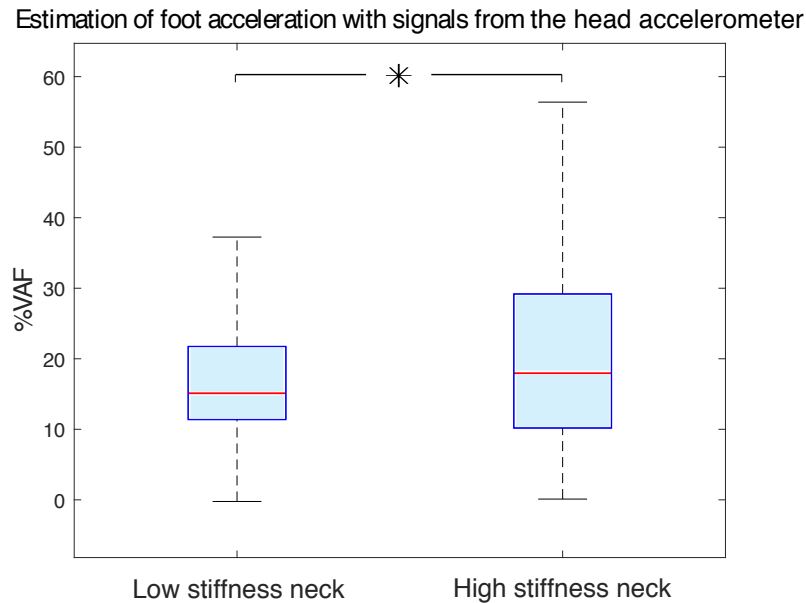


Figure 8. Estimation accuracy of foot acceleration as a function of neck type. Increasing neck stiffness improved estimation of foot acceleration from acceleration measured at the head. Low stiffness and high stiffness neck data were statistically different ($p < 0.05$). The median %VAF was 15.11 and 17.95 for the low stiffness neck and high stiffness neck respectively.

242 There are limitations to our approach that, while worth mentioning, we believe do not challenge the
 243 validity of our results. Importantly, our physical model can only approximate the anatomy and muscle
 244 mechanics of the guinea fowl. Our multi-link articulated structure approximates only the general link-
 245 segment arrangement and length proportions of the animal skeleton, and the viscoelastic rubber bands
 246 only roughly approximate the properties of muscle-tendon linkages. Similarly, we did not consider the
 247 proprioceptive signals coming from the joints, skin and muscles that could also contribute to state estimates
 248 of foot acceleration. While these limitations prevent us from claiming that our results are direct parallels of
 249 how a guinea fowl would respond neuro-mechanically to perturbations, it is nevertheless a valid means to
 250 *test for differences in sensory signals as a function of sensor location and neck stiffness*. Moreover, we
 251 explicitly avoided making the assumption that the skeleton of the guinea fowl was simply a set of links
 252 rigidly fused at a given posture. Rather, we used rotating hinges at the joints, where the posture of the model
 253 was achieved by appropriately setting the lengths and tensions of the rubber bands to approximate muscle-
 254 tendon actions to maintain posture at rest. This mechanical structure—as a first approximation—provides a
 255 biomechanically realistic instantaneous response to a perturbation at the feet, and avoids other multiple
 256 assumptions associated with a computational model [21]. The results we present here are an analysis of the
 257 aggregate acceleration responses to a sequence of center-out 3-dimensional perturbations. As such, we
 258 consider the details of each response only implicitly. Future research could explore the moment-to-moment
 259 details of the responses within an individual perturbation.

260 The biological interpretation of these results hinges on the assumption that the functional benefits of
 261 hip-localized balance sense could translate into selective evolutionary pressure to promote the anatomical
 262 specialization of the LSO in evolutionary time. This assumption is supported by two fundamental control-
 263 theoretical notions: (i) that delays are detrimental because they make any causal closed-loop controller

264 (biological or engineered) more unstable [22] and (ii) that having a more faithful estimate of a perturbation
265 improves the corrective response, and thus improving performance, economy and stability.

266 The simplest interpretation of the time delays hinges on the notion that a causal feedback controller has
267 knowledge of the past, but not of the present (strictly speaking) or future. Therefore, it cannot execute
268 anticipatory control actions and is thus limited by its closed-loop bandwidth. In contrast, biological
269 systems are well-known to produce anticipatory motor commands [23, 24], as well as short-latency
270 reflexive responses [25, 26, 27]. Anticipatory strategies are considered to be critical adaptations to mitigate
271 the deleterious effects of large transmission and processing delays inherent to neural systems [28, 29].
272 Nevertheless, any voluntary, anticipatory or reflexive action would benefit from shorter delays. This point is
273 supported by the observation of many morphological and physiological adaptations in the nervous systems
274 to reduce time delays such as increased axonal diameter, myelination and saltatory conduction.

275 The biological relevance of state estimation [30, 31] relates to the fact that physiological sensory signals
276 contain task-relevant information, but not necessarily in the coordinates and units used by the controller. In
277 particular, some version of the ‘state’ of the system is encoded in sensory coordinates and units that are
278 different from those used by the neural controller to select, plan and execute a response. This means that any
279 raw sensory signal (e.g., acceleration at the LSO or vestibular system) must first be interpreted to extract
280 useful information (e.g., the details of the perturbation at the feet). The MOESP state-space identification
281 technique is but one example of a state estimator [16, 17]. To test our hypothesis, it suffices to show that a
282 hip-localized balance sensing organ is better at sensing, estimating, *and reconstructing* the perturbations
283 at the feet than a head-localized one, Figure 6. On the same figure, we only show forward/backward
284 accelerations (i.e., along the y axis), which are the most destabilizing during locomotion. It has been shown
285 that lateral (i.e., side-to-side) movements are more stable than forward/backward movements because
286 stance width naturally provides a stabilizing effect [32]. Whether and how the concept of state estimation
287 applies to the nervous system, however, is yet unresolved [33].

288 Necker stated in the concluding paragraph of his 2006 paper that ‘The local organization of the neuronal
289 network [of the LSO] favors rapid and hence effective control,’ with no further elaboration [2]. We now
290 present what is, to the best of our knowledge, the first concrete evidence that a hip-localized balance sense
291 organ (like the LSO) is an effective source of *faster* and *better* sensing of posture-relevant information.
292 Faster sensing is evidenced by the shorter time delays for hip-localized vs. a head-localized accelerometers.
293 Moreover, our results also show that the time delays for head-localized balance sense organs can be
294 shortened by cocontracting neck muscles (i.e., a stiffer neck). From the state estimation point of view,
295 however, we find that hip-localized balance sense organs are superior, and do not benefit from sensory
296 fusion with head-localized acceleration—independently of neck stiffness. Therefore, we conclude that
297 hip-localized balance sense indeed promotes more rapid and effective control.

298 These results have important implications for how the evolution of hip-localized balance sense by the
299 LSO might have contributed to the unique sensorimotor control features of birds. In particular, it has long
300 been recognized that birds have relatively ‘modular’ function and control of wings, legs and tail compared
301 to other vertebrates [34]. The functional dissociation between forelimb (wing) for aerial locomotion
302 and hindlimb (leg) for terrestrial locomotion is paralleled by increased autonomy of their respective
303 sensorimotor control networks [35, 36, 37, 38, 6]. The presence of a local and distributed balance sensing
304 organ that is directly integrated with hindlimb spinal networks has likely contributed to this modular control
305 organization. The mechanosensing neurons of the LSO project directly to pre-motor neurons in the spinal
306 cord [2, 39]. This suggests the balance sense information produced by the LSO is likely to contribute to

307 rapid and effective control because it is processed locally. Such local processing is advantageous because
308 involving the brain in the response could introduce counterproductive time delays.

309 While our results focus on perching, hip-localized balance sense is likely beneficial for other postural
310 and locomotor tasks. We designed our perturbations to simulate sensory inputs analogous to bird perching
311 on a branch subject to varied 3-D movements such as wind, movements of other animals, etc. During
312 perching, a bird is exposed to 3-D substrate perturbations, for which short-latency reflex responses could
313 suffice, if sufficiently rapid sensing is available. This is similar to the observed knee and ankle strategies in
314 the control of human upright posture [40], or slip-grip mechanisms for human finger manipulation [41].
315 Moreover, such rapid and informative sensing is also critical to low-level (distributed, spinal or sub-cortical)
316 sensorimotor processing to control short-latency responses to perturbations [42, 43] that ultimately supports
317 long-latency control of voluntary function in general. The LSO is directly integrated with the hindlimb
318 spinal motor control networks [2, 39], suggesting that hip-localized balance sense is likely relevant to all
319 hindlimb-mediated behaviours, including perching, standing balance, over-ground locomotion and arboreal
320 locomotion. Birds effectively have two distinct balance sensorimotor processing centers: the ‘cerebral
321 brain’, responsible for executive function and navigation, and the ‘sacral brain’, responsible for low-level,
322 short latency control of terrestrial perching, standing and locomotion.

323 Adopting lessons from the millions of years of biological evolution poses intriguing and exciting
324 possibilities for the *engineering* evolution of robust and versatile bipedal robots. There are well known
325 forms of morphological control where the structure of the body co-evolves with the nervous system (or
326 controller) to simplify and improve open- or closed-loop control [4, 44, 45]. At the other extreme we
327 have the classical robotics approach to fully centralized control that depends on algorithms that process
328 sensory information and issue motor commands. The LSO provides support for an intermediate alternative,
329 where one can have the benefits of morphological adaptations and central control— but supplemented by
330 distributed neural control centers informed by distributed balance sense organs like the LSO.

4 CONFLICT OF INTEREST STATEMENT

331 The authors declare that the research was conducted in the absence of any commercial or financial
332 relationships that could be construed as a potential conflict of interest.

5 AUTHOR CONTRIBUTIONS

333 DU designed and constructed the physical model of the guinea fowl, wrote the Title, Abstract, Introduction,
334 did renders of the physical model of the guinea fowl and put together different author ideas and perspectives.

335 KJ guided the NI DAQ implementation and data analysis activities: system identification analysis,
336 bootstrap analysis and statistics.

337 Together, DU and KJ implemented the NI DAQ system, programmed the AdeptSix 300 robotic arm, did
338 data analysis on MATLAB, wrote the Methods section created and edited the figures.

339 MD and FV gave the initial idea of giving an engineering quantitative analysis for functional benefits of
340 the LSO balance sense in birds. They wrote most of the Discussion section and validated: (i) the design
341 and construction of the physical model of the guinea fowl, (ii) data analysis activities and (iii) each of the
342 paper sections and figures.

343 All the authors contributed to editing the paper for style, clarity, succinctness and grammar.

6 FUNDING

344 Research reported in this publication was supported by the National Institute of Arthritis and
345 Musculoskeletal and Skin Diseases of the National Institutes of Health under Awards Number R01
346 AR-050520 and R01 AR-052345, and by the Department of Defense under award number MR150091 to
347 F.V-C. The content of this endeavor is solely the responsibility of the authors and does not necessarily
348 represent the official views of the National Institutes of Health or the Department of Defense. This work
349 was also supported by Fonds Québécois de la Recherche sur la Nature et les Technologies to KJ.

ACKNOWLEDGMENTS

350 Author MD would like to thank Alexander Spröwitz for discussions on the potential balance sensing
351 function of the lumbosacral organ of birds.

REFERENCES

- 352 [1]Monique Maurice, Henri Gioanni, and Anick Abourachid. Influence of the behavioural context on the
353 optocollic reflex (OCR) in pigeons (*Columba livia*). *Journal of experimental biology*, 209(2):292–301,
354 2006.
- 355 [2]Reinhold Necker. Specializations in the lumbosacral vertebral canal and spinal cord of birds: evidence
356 of a function as a sense organ which is involved in the control of walking. *Journal of Comparative*
357 *Physiology A*, 192(5):439, 2006.
- 358 [3]R Necker. The structure and development of avian lumbosacral specializations of the vertebral canal
359 and the spinal cord with special reference to a possible function as a sense organ of equilibrium.
360 *Anatomy and embryology*, 210(1):59–74, 2005.
- 361 [4]Ashley E Pete, Daniel Kress, Marina A Dimitrov, and David Lentink. The role of passive avian head
362 stabilization in flapping flight. *Journal of The Royal Society Interface*, 12(110):20150508, 2015.
- 363 [5]Reinhold Necker. Head-bobbing of walking birds. *Journal of comparative physiology A*, 193(12):1177,
364 2007.
- 365 [6]Kimberly L McArthur and J David Dickman. State-dependent sensorimotor processing: gaze and
366 posture stability during simulated flight in birds. *Journal of neurophysiology*, 105(4):1689–1700, 2011.
- 367 [7]Anick Abourachid, Remi Hackert, Marc Herbin, Paul A Libourel, François Lambert, Henri Gioanni,
368 Pauline Provini, Pierre Blazevic, and Vincent Hugel. Bird terrestrial locomotion as revealed by 3D
369 kinematics. *Zoology*, 114(6):360–368, 2011.
- 370 [8]Miomir Vukobratovic, Branislav Borovac, Dusan Surla, and Dragan Stokic. *Biped locomotion:*
371 *dynamics, stability, control and application*, volume 7. Springer Science & Business Media, 2012.
- 372 [9]George L Streeter. The structure of the spinal cord of the ostrich. *Developmental Dynamics*, 3(1):1–27,
373 1904.
- 374 [10]DM Schroeder and RG Murray. Specializations within the lumbosacral spinal cord of the pigeon.
375 *Journal of Morphology*, 194(1):41–53, 1987.
- 376 [11]Yuko Yamanaka, Naoki Kitamura, and Izumi Shibuya. Chick spinal accessory lobes contain functional
377 neurons expressing voltagegated sodium channels generating action potentials. *Biomedical Research*,
378 29(4):205–211, 2008.
- 379 [12]Anne Lill Eide and Joel C Glover. Development of an identified spinal commissural interneuron
380 population in an amniote: neurons of the avian hofmann nuclei. *Journal of Neuroscience*, 16(18):5749–
381 5761, 1996.

- 382 [13]Monica A Daley, G Felix, and Andrew A Biewener. Running stability is enhanced by a proximo-distal
383 gradient in joint neuromechanical control. *Journal of Experimental Biology*, 210(3):383–394, 2007.
- 384 [14]SM Gatesy and AA Biewener. Bipedal locomotion: effects of speed, size and limb posture in birds and
385 humans. *Journal of Zoology*, 224(1):127–147, 1991.
- 386 [15]Joanne C Gordon, Jeffery W Rankin, and Monica A Daley. How do treadmill speed and terrain
387 visibility influence neuromuscular control of guinea fowl locomotion? *Journal of Experimental*
388 *Biology*, 218(19):3010–3022, 2015.
- 389 [16]Michel Verhaegen and Vincent Verdult. *Filtering and system identification: a least squares approach*.
390 Cambridge university press, 2007.
- 391 [17]Michel Verhaegen and Patrick Dewilde. Subspace model identification part 1. the output-error state-
392 space model identification class of algorithms. *International journal of control*, 56(5):1187–1210,
393 1992.
- 394 [18]Bert Haverkamp and Michel Verhaegen. Smi toolbox: State space model identification software for
395 multivariable dynamical systems. *Delft University of Technology, Delft, The Netherlands*, 1997.
- 396 [19]Bert Haverkamp. *Subspace method identification, theory and practice*. PhD thesis, PhD thesis, TU
397 Delft, Delft, The Netherlands, 2000.
- 398 [20]Bradley Efron and Robert J Tibshirani. *An introduction to the bootstrap*. CRC press, 1994.
- 399 [21]Flávio VC Martins, Eduardo G Carrano, Elizabeth F Wanner, Ricardo HC Takahashi, and Geraldo R
400 Mateus. A dynamic multiobjective hybrid approach for designing wireless sensor networks. In
401 *Evolutionary Computation, 2009. CEC'09. IEEE Congress on*, pages 1145–1152. IEEE, 2009.
- 402 [22]Keqin Gu, Jie Chen, and Vladimir L Kharitonov. *Stability of time-delay systems*. Springer Science &
403 Business Media, 2003.
- 404 [23]Alexander S Aruin and Mark L Latash. The role of motor action in anticipatory postural adjustments
405 studied with self-induced and externally triggered perturbations. *Experimental Brain Research*,
406 106(2):291–300, 1995.
- 407 [24]David T Westwick and Eric J Perreault. Closed-loop identification: application to the estimation
408 of limb impedance in a compliant environment. *IEEE Transactions on Biomedical Engineering*,
409 58(3):521–530, 2011.
- 410 [25]Thomas Sinkjær, Jacob Buus Andersen, Jørgen Feldbæk Nielsen, and Hans Jacob Hansen. Soleus
411 long-latency stretch reflexes during walking in healthy and spastic humans. *Clinical Neurophysiology*,
412 110(5):951–959, 1999.
- 413 [26]Kian Jalaieddini, Ehsan Sobhani Tehrani, and Robert E Kearney. A subspace approach to the structural
414 decomposition and identification of ankle joint dynamic stiffness. *IEEE transactions on biomedical*
415 *engineering*, 64(6):1357–1368, 2017.
- 416 [27]Kian Jalaieddini, Chuanxin Minos Niu, Suraj Chakravarthi Raja, Won Joon Sohn, Gerald E Loeb,
417 Terence D Sanger, and Francisco J Valero-Cuevas. Neuromorphic meets neuromechanics, part ii: the
418 role of fusimotor drive. *Journal of neural engineering*, 14(2):025002, 2017.
- 419 [28]Bruce P Bean. The action potential in mammalian central neurons. *Nature Reviews Neuroscience*,
420 8(6):451–465, 2007.
- 421 [29]A Aldo Faisal, Luc PJ Selen, and Daniel M Wolpert. Noise in the nervous system. *Nature reviews*
422 *neuroscience*, 9(4):292–303, 2008.
- 423 [30]Rudolph Emil Kalman et al. A new approach to linear filtering and prediction problems. *Journal of*
424 *basic Engineering*, 82(1):35–45, 1960.
- 425 [31]Dan Simon. *Optimal state estimation: Kalman, H infinity, and nonlinear approaches*. John Wiley &
426 Sons, 2006.

- 427 [32]Jesse C Dean, Neil B Alexander, and Arthur D Kuo. The effect of lateral stabilization on walking in
428 young and old adults. *IEEE Transactions on Biomedical Engineering*, 54(11):1919–1926, 2007.
- 429 [33]Gerald E Loeb. Optimal isn't good enough. *Biological cybernetics*, 106(11-12):757–765, 2012.
- 430 [34]Stephen M Gatesy and Kenneth P Dial. Locomotor modules and the evolution of avian flight. *Evolution*,
431 50(1):331–340, 1996.
- 432 [35]Stephen Ho and Michael J O'Donovan. Regionalization and intersegmental coordination of rhythm-
433 generating networks in the spinal cord of the chick embryo. *Journal of Neuroscience*, 13(4):1354–1371,
434 1993.
- 435 [36]Gerald N Sholomenko and John D Steeves. Effects of selective spinal cord lesions on hind limb
436 locomotion in birds. *Experimental neurology*, 95(2):403–418, 1987.
- 437 [37]Richard D Jacobson and M Hollyday. Electrically evoked walking and fictive locomotion in the chick.
438 *Journal of Neurophysiology*, 48(1):257–270, 1982.
- 439 [38]Marguerite Biederman-Thorson and John Thorson. Rotation-compensating reflexes independent of the
440 labyrinth and the eye. *Journal of comparative Physiology*, 83(2):103–122, 1973.
- 441 [39]Anne Lill Eide. The axonal projections of the hofmann nuclei in the spinal cord of the late stage
442 chicken embryo. *Anatomy and embryology*, 193(6):543–557, 1996.
- 443 [40]Jeffrey T Bingham, Julia T Choi, and Lena H Ting. Stability in a frontal plane model of balance requires
444 coupled changes to postural configuration and neural feedback control. *Journal of neurophysiology*,
445 106(1):437–448, 2011.
- 446 [41]Kelly J Cole and James H Abbs. Grip force adjustments evoked by load force perturbations of a
447 grasped object. *Journal of neurophysiology*, 60(4):1513–1522, 1988.
- 448 [42]Emily L Lawrence, Guilherme M Cesar, Martha R Bromfield, Richard Peterson, Francisco J Valero-
449 Cuevas, and Susan M Sigward. Strength, multijoint coordination, and sensorimotor processing are
450 independent contributors to overall balance ability. *BioMed research international*, 2015, 2015.
- 451 [43]Emily L Lawrence, Sudarshan Dayanidhi, Isabella Fassola, Philip Requejo, Caroline Leclercq,
452 Carolee J Winstein, and Francisco J Valero-Cuevas. Outcome measures for hand function naturally
453 reveal three latent domains in older adults: strength, coordinated upper extremity function, and
454 sensorimotor processing. *Frontiers in aging neuroscience*, 7, 2015.
- 455 [44]Hod Lipson and Jordan B Pollack. Automatic design and manufacture of robotic lifeforms. *Nature*,
456 406(6799):974–978, 2000.
- 457 [45]Francisco J Valero-Cuevas, Jae-Woong Yi, Daniel Brown, Robert V McNamara, Chandana Paul, and
458 Hod Lipson. The tendon network of the fingers performs anatomical computation at a macroscopic
459 scale. *IEEE Transactions on Biomedical Engineering*, 54(6):1161–1166, 2007.